

Development of Thin-type Ultrasonic Motors for High-speed Applications – Mainly Lead-free Single-Crystal-type –

Manabu Aoyagi

Muroran Institute of Technology
Muroran, Hokkaido 050-8585
maoyagi@mmm.muroran-it.ac.jp

Takehiro Takano

Tohoku Institute of Technology
Sendai, 982-8577
ktakano@tohtech.ac.jp

Hideki Tamura

Yamagata University
Yonezawa, Yamagata 992-8510
htamura@yz.yamagata-u.ac.jp

Yoshiro Tomikawa, and Seiji Hirose

Yamagata University
Yonezawa, Yamagata 992-8510
{tomikawa/hirose}@yz.yamagata-u.ac.jp

Abstract— Several types of high-speed ultrasonic motor have been proposed and evaluated experimentally by the authors. Usually, high torque at low speed is one of major special features of an ultrasonic motor. However, they have a possibility on high-speed applications and advantages of input power and thin structure to ordinal electromagnetic motors. This paper mainly deals with constructions and experimental results of a single crystal ultrasonic motor. Good high-speed characteristics are obtained.

I. INTRODUCTION

AN ultrasonic motor can produce a high torque at a low speed, so that it is not necessary to use gears, and direct drive is possible. This is one of the major features of an ultrasonic motor (USM). However, if a load is a little light and a constant high-speed revolution is required as uses in a disk drive or a micro fan, high torque is not necessary.

In recent years, the reduction in size of portable electric equipments has been demanded, and equipped spindle motors are also required to be more compact and improved in performance. A thin electromagnetic d.c. motor (DCM) has been widely used in these applications. However, it is not easy to thin DCMs less than 1mm within the necessary performance. On the contrary, as there is flexibility in choosing the shape of USM, some types are suitable to be made less than 1mm thickness. Small USMs are able to yield mechanical output power greater than an electromagnetic motor of similar size.

From the viewpoint of their shapes, USMs can be selected or designed for more suitable applications. If USMs can revolve faster over a long-time continuous operation, its application would spread widely. This study is a response to new challenges of developing a new field of applications of USMs. The above stated backgrounds are the motivation of this study.

The authors have proposed several types of a high-speed USM using piezoelectric ceramics and single crystal LiNbO_3 , as described in section II. This paper mainly deals with design concepts and experimental results of a single crystal

high-speed USM.

II. CONCEPT AND INVESTIGATED ITEMS

Research projects of thin-type high-speed ultrasonic motor are based on the following design concepts, and several types of a thin USM have been considered as shown in Table I.

A) Small volume, simple structure and simple drive: USMs and its drive circuit used in portable electric equipments are required to reduce their volume as much as possible. Hence a single-phase-drive motor is suitable for saving an occupied space. Some single-phase-drive motors using a longitudinal vibration or flexural one of the thin plate-type of stator vibrator are proposed and experimented^[1].

B) Low drive voltage (multilayer ceramics): Portable electric equipments require the operation in low drive voltage. Multilayer structure piezoceramics can reduce the drive voltage. A single-phase-drive motor using diagonally symmetrical multilayered ceramic plate is examined^[2].

C) Lead-free (LiNbO_3 rectangular plate USM): Ordinal piezoelectric ceramics (PZT) which is widely used in many applications contain lead, but a lead-free has been being required. As one of solution of lead-free, stator vibrators using LiNbO_3 which is piezoelectric single crystal are proposed and experimented^[3].

D) New operating principle (Gyro-moment motors): It is not necessary to be particular about a friction drive as an ultrasonic motor. A new operating principle using a gyro-moment generated by vibrations is proposed^[4-7].

TABLE I DESIGN CONCEPTS AND MOTORS CONSIDERED IN THIS PROJECT

Concept and Item	1) Simple drive & structure	2) Low drive voltage	3) Lead free	4) New operating principle
A: PZT plate with shim	⊙			
B: Multilayer ceramics	⊙	⊙		
C: Single crystal (LiNbO_3)	⊙		⊙	
D: Gyro-moment motor	○	○	○	⊙

An operating principle and examination results of rectangular single crystal USM are described below.

III. MOTOR TYPE C: PIEZOELECTRIC SINGLE CRYSTAL ULTRASONIC MOTOR USING LiNbO_3

Several crystal ultrasonic motors described in Table II have been studied. For miniature motor, especially we propose a single-phase drive motor using coupling modes caused by a double rotated Y-cut rectangular plate.

A. Mode coupling caused by crystal second rotation

An X-rotated Y-cut plate of LiNbO_3 as shown in Fig. 1(a) can strongly excite in-plane vibrations by the piezoelectric transverse effect at the X-rotation angle θ ranging from 120° to 160° . The X-rotated rectangular plate aligned with the z' - and x -axis has a pure longitudinal first and a flexural second vibration modes; and their internal strains are shown in Fig. 2. The both modes are independent and cannot be used as the single-phase motor.

However, applying a second rotation Φ in the y' -axis to the rectangular plate vibrator as shown in Fig. 1(b), the longitudinal and flexural vibrations are coupled. Accordingly, two coupling modes are obtained as shown in Fig. 3. The coupling mode with the higher resonance frequency is called the upper mode, and the other is called the lower mode in this study. It is different in displacement directions at the center point of a tip of the vibrator between the both modes illustrated in Fig. 3; therefore, mode switching inverts the direction of rotor revolution.

It should be noted that the elastic compliances s_{15}^E , s_{25}^E and s_{35}^E are not zero when the second rotation angle Φ is not 0 and 90° . For example, $\theta = 135^\circ$, their values as functions of Φ are shown in Fig. 4. The compliances combine stresses and strains between the longitudinal and flexural vibrational components.

In these vibration modes, the tensile strain S_3 in length has the largest value; and the value of s_{35}^E is important to design of the vibrator for strong coupling. Therefore, the angle Φ around 15° is acceptable.

Table II Background of the studies for ultrasonic motors using LiNbO_3 plates.

Vibrator shape	Vibration modes	Driving
Rectangular	Longitudinal 1st, Flexural 2nd	Two phase
Square	Same form double flexural mode	Two phase
Parallelogram	Coupling modes	Single
Double rotated rectangular	Coupling modes	Single

Dimensions of the vibrator are defined by FEM analysis to obtain symmetric displacement form between the upper and lower modes, and the dimensions of a sample vibrator are $10 \times 2.55 \times 0.25 \text{ mm}^3$ and $\theta = 140^\circ$ and $\Phi = 14^\circ$.

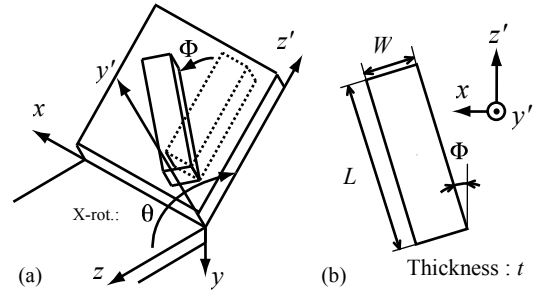


Fig. 1 X-rotated Y-cut LiNbO_3 plate with Y' -rotation.

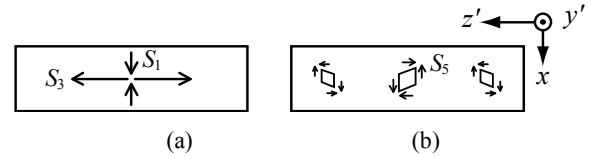


Fig. 2 Tensile strains S_1 and S_3 in 1st longitudinal mode (a), and in-plane shear strain S_5 in 2nd flexural mode (b).

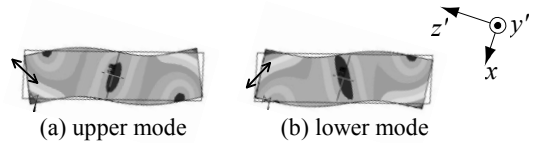


Fig. 3 Coupling modes in a double rotation Y-cut plate.

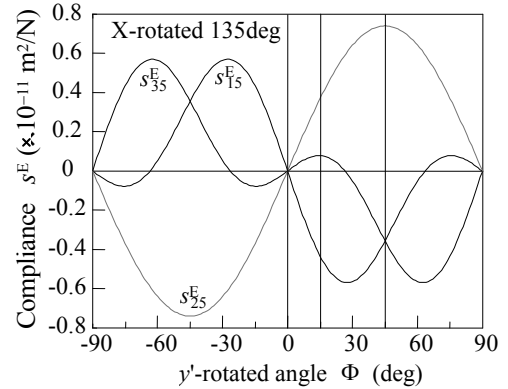


Fig. 4 Elastic compliances s_{35}^E , s_{15}^E and s_{25}^E as functions of second rotation angle Φ .

B. Motor construction and measurement

Experimental vibrators are sawed off from a wafer after mirror-polished and evaporated Cr/Au electrodes on both sides of the entire y' -face. The design of a trial stator is shown in Fig. 5. The common nodes of both the upper and lower modes are located in the center points on the top and bottom surfaces of the vibrator, and they are supported by metal pins 0.5 mm in diameter with a conductive adhesive material. The pins combine the role of support with the role of an electric supply line to eliminate additional feeder cables and its mechanical load.

The measurement system used is shown in Fig. 6. The stator vibrator described is attached to a linear slider table, and a preload force is applied that is monitored with a force meter. The preloaded stator contacts a rotor which consists of a code

wheel and a thin stainless steel shaft of 1 mm diameter. The code wheel and an optical encoder emit 360 pulses per revolution, and a recorder counts the pulses in 2 ms increments to obtain the revolution speed. The torque of this motor is too small to measure directly. Therefore, load characteristics are estimated from the transient responses of the revolution speed and the input electric power.

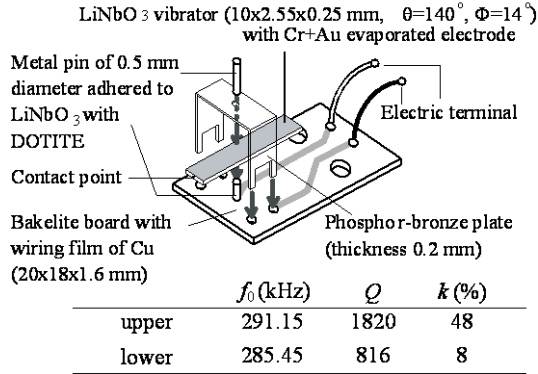


Fig. 5 Support configuration of stator vibrator.

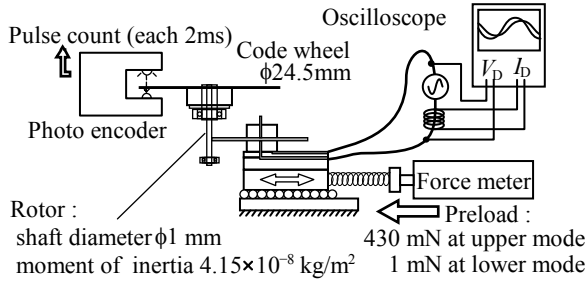
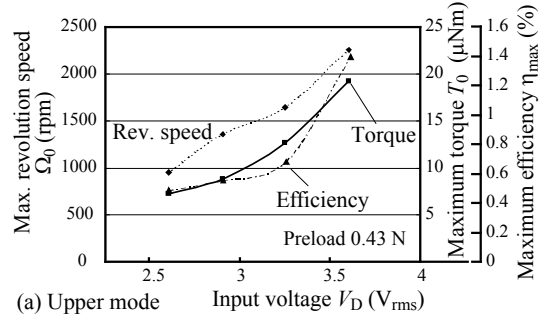


Fig. 6 Measurement system.

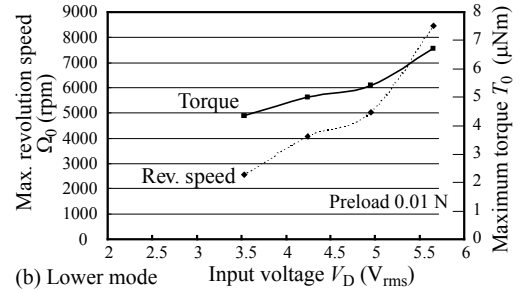
C. Experimental results

The directions of rotation are CCW in the upper mode and CW in the lower mode; therefore, the reverse operation is obtained by the driving mode change. However, the amount of preload when the motor can rotate is in the range from 0.3 to 0.8 N in the upper mode, whereas the rotatable range is from 0.01 to 0.09 N in the lower mode. The difference in the rotatable range of preload is a problem for the actual operation of the directional change. Furthermore, the motor performance also differs between using the upper and lower modes as shown in Fig. 7; the characteristics show a relatively low-speed and high-torque using the upper mode, and the opposite characteristics with the lower mode. For example, using the upper mode, the maximum revolution speed is 2200 rpm and the maximum torque is 19 μ Nm when 3.6 V is applied. On the other hand, using the lower mode, the maximum speed is 7500 rpm and the maximum torque is 6.5 μ Nm when 5.5 V is applied.

We considered that the influence of the support and preload-force changes the shape of the vibration from the state in the analysis, and the upper and lower mode shift to longitudinal and flexural ascendant modes, respectively. Details of this influence will be examined in future work.



(a) Upper mode



(b) Lower mode

Fig. 7 Rotation characteristics.

D. Load characteristics in low speed with thick shaft

Above structure with the thin shaft shows high speed and very low torque characteristics. An increase in the shaft diameter decreases the revolution speed and increases the torque. Therefore, we also measured load characteristics using a system as shown in Fig. 8. The system used a shaft of 5 mm diameter and loaded by a friction of a string tensioned with a weight. In this measurement, the dimensions of LiNbO₃ vibrator used are 10x2.55x0.5 mm³ and $\theta=135^\circ$ and $\Phi=14^\circ$, and its equivalent circuit constants of the upper and lower mode are shown in Table III.

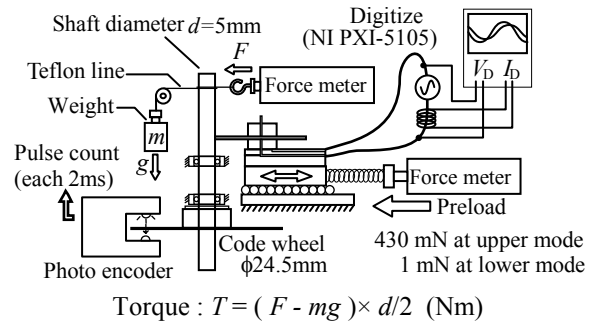


Fig. 8 Measurement system for load characteristics.

Table III Equivalent circuit constants for X135°- and Y14°-rotated Y-cut rectangular plate. (10x2.55x0.25 mm)

Mode	Upper	Lower
Q	780	1816
f_0 (kHz)	288.62	283.22
R (Ω)	408.8	181.7
L (mH)	175.9	185.3
C (pF)	1.73	1.70
C_d (pF)	28.0	27.9
k (%)	40.7	12.3

Figures 9 and 10 show characteristics of revolution speed as function of the driving frequency without the load tension. The frequency characteristic in the upper mode has a hysteresis curve, and the motor cannot be started up at a frequency out of the start range as shown in Fig. 9. However, the maximum revolution speed is obtained at a driving frequency lower than the start range frequency. Therefore, to operate at high speed in low driving voltage, we have to make a frequency control driver.

On the other hand, the hysteresis characteristic is not prominently observed in the lower mode. Using the lower mode can rotate the shaft inverse direction from the upper mode used operation. However, the rotation direction does not invert when the driving frequency is around 290 kHz, and fluctuates in range from about 286 to 290 kHz. Additionally, the motor sounds friction noise when it is driven outside the frequency range from 284.5 to 285.5kHz. Hence, the lower mode can be stably used in narrow range of the frequency.

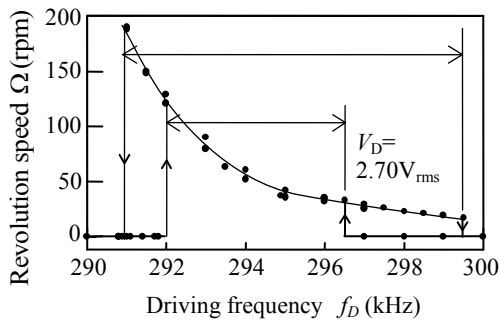


Fig. 9 Hysteresis characteristic of revolution speed using upper mode when no-load operation.

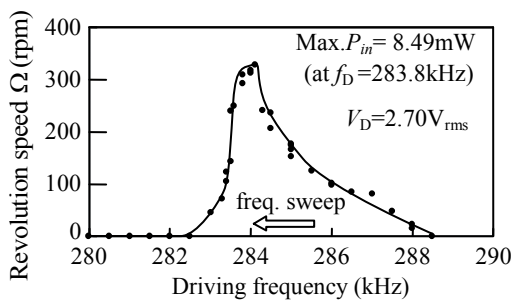


Fig. 10 Revolution speed as function of driving frequency using lower mode when no-load operation.

When a driving frequency is selected at the center of the start range, load characteristics using the upper mode are shown in Fig. 11. Increasing the load torque until 45 μNm decreases the speed gradually and increases the efficiency. However, when the torque exceeds 45 μNm , the motor alternates between run and stop; thus, the revolution is unstable and cannot be measured.

Figure 12 shows load characteristics when the driving frequency is 285 kHz for the lower mode with noiseless revolution. The efficiency is higher in a low torque region. The speed decreases steeply with increasing the torque. Therefore, this driving condition is sensitive to the load.

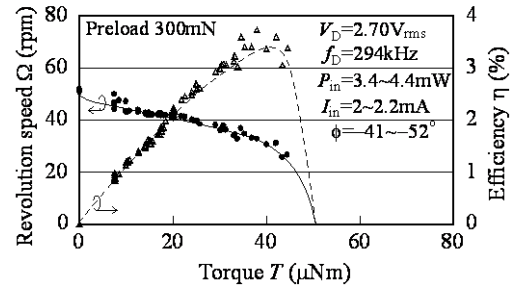


Fig. 11 Load characteristic for the upper mode.

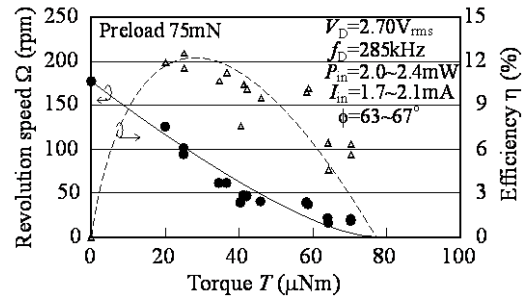


Fig. 12 Load characteristic for the lower mode.

IV. CONCLUSION

High-speed ultrasonic spindle motors using several types of a stator vibrator can be easily realized in an initial level. Considering the practical use of this type of motor, problems concerning durability and stability, which are greatly influenced by the wear of a friction surface, must be solved.

ACKNOWLEDGMENT

This research was partially supported by the Ministry of Education, Culture, Sports, Science and Technology, Grant in-Aid for Scientific Research on Priority Areas (No.438) No.19016001.

REFERENCES

- [1] M. Aoyagi, F. Suzuki, Y. Tomikawa and I. Kano, "High Speed Thin Ultrasonic Spindle Motor and Its Application," *Jpn.J.Appl.Phys.*, vol.43, no.5B, pp. 2873-2878, 2004.
- [2] M. Aoyagi and Y. Tomikawa: "Ultrasonic Motor Based on Coupled Longitudinal-Bending Vibrations of a Diagonally Symmetric Piezoelectric Ceramic Plate," *Electronics and Communications in Japan*, vol.79, 6, pp.60-67, 1996.
- [3] H. Tamura, K. Kawai, T. Takano, Y. Tomikawa, S. Hirose and M.Aoyagi: "A Diagonally Symmetric Form Ultrasonic Motor Using a LiNbO₃ Plate," *Jpn.J.Appl.Phys.*, vol.46, no.7B, pp.4698-4703, 2007.
- [4] K.Kanauchi and Y.Tomikawa, ACTUATOR 2000. 7th International Conference on New Actuator, 19-21 June 2000, Bremen, Germany, No.B2.2, pp.246-249, 2000.
- [5] Y.Tomikawa and Y.Matsuzaka, ACTUATOR 2002. 8th International Conference on New Actuator, 10-12 June 2002, Bremen, Germany, No.P15, pp.450-453, 2002.
- [6] Y.Tomikawa, T.Takano and M.Aoyagi, 2005 IEEE Ultrasonic symposium, 18-21 September 2005, Rotterdam, Netherland, No.P1H-7, pp.1526-1529, 2005.
- [7] Y.Tomikawa, C.Kusakabe, T.Takano, M.Aoyagi and H.Tamura, ACTUATOR 2006. 10th International Conference on New Actuator, 14-16 June 2006, Bremen, Germany, pp.576-579, 2006.